INTERNATIONAL JOURNAL OF SATELLITE COMMUNICATIONS AND NETWORKING
Int. J. Satell. Commun. Network. 2017; **00**:1–21
Published online in Wiley InterScience (www.interscience.wiley.com). DOI: 10.1002/sat

Adaptive Frequency Hopping Schemes for CR-based Multi-link Satellite Networks

Irmak Aykin, Marwan Krunz, and Yong Xiao

Department of Electrical and Computer Engineering, University of Arizona, Tucson, AZ 85721, USA

SUMMARY

In this paper, we study two dynamic frequency hopping (DFH)-based interference mitigation approaches for satellite communications. These techniques exploit the sensing capabilities of a cognitive radio (CR) to predict future interference on the upcoming frequency hops. We consider a topology where multiple low Earth orbit (LEO) satellites transmit packets to a common geostationary equatorial orbit (GEO) satellite. The FH sequence of each LEO-GEO link is adjusted according to the outcome of out-of-band proactive sensing scheme, carried out by a CR module in the GEO satellite. Based on sensing results, new frequency assignments are made for the upcoming slots, taking into account the transmit powers, achievable rates, and overhead of modifying the FH sequences. In addition, we ensure that all satellite links are assigned channels such that their minimum signal-to-interference-plus-noise ratio (SINR) requirements are met, if such an assignment is possible. We formulate two multi-objective optimization problems: DFH-Power and DFH-Rate. Discrete-time Markov chain analysis is used to predict future channel conditions, where the number of states are inferred using k-means clustering and the state transition probabilities are computed using maximum likelihood estimation. Finally, simulation results are presented to evaluate the effects of different system parameters on the performance of the proposed designs.

Received . . .

KEY WORDS: Cognitive radio; dynamic frequency hopping; maximum likelihood estimation; Markov models; out-of-band sensing; satellite communications.

1. INTRODUCTION

RF interference can significantly degrade the performance of satellite networks. To cope with that, spreading systems are often used as the first "line of defense" against active (jamming) and passive (eavesdropping) attacks [1]. In direct sequence (DS) spread spectrum, the signal is passed through a spreading function and distributed over the entire band at once. On the other hand, in frequency hopping (FH) spread spectrum, the carrier frequency of the signal is switched between a set of frequencies using a pseudorandom noise (PN) sequence. Even though both approaches tend to work well against eavesdroppers, FH spread spectrum is more robust to interferers than DS spread spectrum. Some examples of satellite systems that employ FH include the Advanced Extremely High Frequency (AEHF) [2] and the Military Strategic and Tactical Relay (MILSTAR) satellite systems [3]. Indeed, FH is extensively used in military satellite systems to secure communications, especially under adversarial conditions [4]. Although traditional FH where the carrier frequencies are changed using a fixed PN sequence tends to work well under random interference, it performs

An abridged version of this paper was presented at the IEEE Globecom 2016 Conference, Washington, DC, December 4-8, 2016.

poorly in the presence of persistent interference over specific channels [5]. For example, if a smart eavesdropper learns parts of the fixed FH sequence, it can persistently target certain frequencies in certain time slots.

One way to address the limitations of the static FH approach is to use dynamic frequency hopping (DFH), in which the FH sequence can be adjusted according to channel quality and interference conditions. DFH was studied in [6] to ensure a certain quality-of-service (QoS) in wireless regional area networks (WRANs) without affecting licensed users. DFH was also used in [5] to combat interference in a single bent-pipe satellite link. The same approach was extended in [7] to multi-link scenarios.

Communications agility in satellite communications (SATCOM) can be significantly enhanced by using cognitive radios (CRs). CRs have the ability to sense the spectrum and adapt the transmission parameters to maximize system capacity while co-existing with legacy wireless radios. Spectrum sensing has been extensively studied for CR applications (see, [8], [9] and the references therein). In [8] several signal processing techniques for spectrum sensing were investigated. In addition, the authors argued that by allowing two or more users to cooperate during spectrum sensing, the sensing accuracy and reliability can be further improved. In [9] the authors discussed the network functions related to spectrum management, spectrum mobility, and spectrum sharing. They also investigated the influence of these functions on the performance of upper-layer protocols, such as routing and transport.

In this paper, we study the use of CRs to improve the robustness of satellite communications. An agile CR platform can improve the performance of a satellite communication system by combating intentional and unintentional interference. CRs for space/satellite communications can be easily built on top of existing software defined radio (SDR) platforms, e.g., SWIFT [10] and General Dynamics (GD) SDR [11]. SWIFT radios are a family of SDRs designed to provide high-performance communications for CubeSats and other small spacecraft. GD SDR, on the other hand, contains a three-million-gate FPGA and can be reconfigured to operate in different modes based on the system requirements. Our designs are mostly targeted to unintentional SATCOM interference where there is no specific jamming pattern. One type of interference that can be alleviated by the proposed methods is the interference caused by antenna pointing errors. In particular, the frequent movement of the antenna platform on satellites may lead to motion-induced antenna pointing errors. Typically, these errors are small and random. Yet, it was shown in [12] that such errors can lead to random variations of the satellites' off-axis EIRP spectral density. As a result, different SATCOM systems operating at the same frequency can interfere with each other. Although the proposed approach is not intended to alleviate intentional interference, certain types of adversarial interference (e.g., an attacker that always jams the same channel, Markovian jammers, etc.) can still be accommodated.

By exploiting the spectrum awareness capabilities of CRs, we investigate two novel DFH schemes for multi-link satellite-to-satellite communications, namely DFH-Rate and DFH-Power. Specifically, we consider communications from multiple low Earth orbit (LEO) satellites to a single geostationary equatorial orbit (GEO) satellite. We study the channel assignment problem assuming that the satellites are capable of DFH. Channel assignment has been widely studied [13][14]. In [14], the problem of assigning channels to CR transmissions was investigated, with the goal of maximizing the number of feasible concurrent CR transmissions. In contrast to [14], in DFH-Power, we aim at simultaneously minimizing the total transmit (Tx) power and changes to the nominal FH sequences while satisfying the signal-to-interference-plus-noise ratio (SINR) requirements of the links. Considering the large distances between LEO and GEO satellites, minimizing the transmit powers is of utmost importance. In addition, minimizing the changes in the nominal FH sequences is beneficial when a feedback channel is not always available/reliable. In DFH-Rate, we aim at maximizing a weighted difference of the total achievable transmission rate (summed over all links) and the overhead of modifying the FH sequences while satisfying SINR requirements of the links.

The main contributions of this paper can be summarized as follows:

DOI: 10.1002/sat

Table I. List of key notation.

Notation	Definition
M	Number of LEO satellites
T	Duration of one slot
$f_j(n)$	Frequency assigned to link j in time slot n
$f_{j,nom}$	Nominal frequency assigned to link j in time slot n
T_s	Sensing time per channel
C	Number of sensed channels in one time slot
T_f	Feedback time
$\mathcal{I}$	Set of channels
$\mathcal{J}$	Set of LEO-GEO links ($\lvert\mathcal{J}\rvert = M$)
D	Lag parameter
$P_j^{(i)}$	Tx power for LEO satellite j communicating over channel i
$P_{\max}$	Maximum allowed Tx power
$\alpha_j^{(i)}$	Binary variable (=1 if channel i is assigned to link j)
β	Weight parameter in the optimization problem
$\text{SINR}_j^{(i)}$	SINR experienced when LEO satellite j communicates over channel i
$R_j^{(i)}$	Rate that LEO satellite j achieves when communicating over channel i
$R_{\max}$	Maximum transmission rate
$w_j^{(i)}$	Weight in the bipartite graph for channel i and link j
Y_n	Total received interference power in slot n
q	Number of states in the DTMC
$z_1, \cdots, z_{q-1}$	State thresholds in the DTMC
k	Number of clusters in the k-means algorithm
S_i	Silhouette value of point i
$\mathbf{A}$	Transition probability matrix of the MC (entries p_{ij})
$x_1, x_2, \cdots, x_v$	Set of observations from the MC
v	Size of observation set
$L(\mathbf{A})$	Likelihood of a transition probability matrix $\mathbf{A}$
$\mathbf{N}$	Transition count matrix (entries n_{ij}) of the MC
$\mathcal{L}(\mathbf{A})$	Log-likelihood of a transition probability matrix $\mathbf{A}$
$\lambda_1, \lambda_2, \cdots, \lambda_q$	Lagrange multipliers to find the MLE of the MC

- We formulate two problems for DFH systems. These problems aim at optimizing different system parameters (total Tx power, overhead, and total rate) and study the trade-off between the terms of the objective functions (power vs. overhead and rate vs. overhead tradeoffs).

- We propose an approach to convert the optimization problems into bipartite matching problems, and we use the low-complexity Hungarian algorithm to solve them.

- Assuming that the interference on a given channel can be modeled as a Markov-chain (MC), we study a method for estimating the parameters of the MC based on k-means clustering and maximum-likelihood estimation (MLE) techniques.

- We analyze the effect of system parameters, including control-packet loss rate and the mean interference power, on the performance of the proposed algorithms.

The remainder of this paper is organized as follows. In Section 2, we introduce our system model. In Section 3, we explain the problem formulations and investigate the trade-off between different objectives. A low-complexity solution for the optimization problems is proposed in Section 4. In Section 5, we present the MC approach for estimating the future channel conditions and in Section 6, we evaluate the performance of our algorithms. Finally, we conclude the paper in Section 7. A list of the key notations used throughout the paper is shown in Table I.

Prepared using satauth.cls
DOI: 10.1002/sat

2. SYSTEM MODEL

The focus of this paper is to develop CR-based DFH methods to alleviate interference from external sources (intentional and unintentional) that cannot be controlled by the GEO and LEO satellites. In our system model, all LEO satellites transmit simultaneously to a common GEO satellite. The GEO satellite knows a priori which LEO satellites will be transmitting, on which channels, and during what time slots. In other words, Each LEO-to-GEO link is pre-assigned a "nominal" FH sequence, drawn from a set of narrowband channels. As a result, interference from other LEO satellites (i.e., intra-system interference) can be easily mitigated by properly scheduling the frequency-hopping patterns among LEO satellites.

Our proposed method consists of two main parts: proactive sensing and channel update. The GEO satellite will first measure the SINR of signals transmitted on each channel during previous time slots. These measurements will then be used to estimate future channel conditions and update the hopping patterns. The LEO satellites are then notified about the changes in the hopping patterns. Received interference could be as a result of other SATCOM systems that are unaware of the existing transmissions between the GEO and LEO satellites, resulting in pointing errors (unintentional interference), or could be caused by unknown sources trying to attack the transmission. Specifically, our method can also accommodate certain types of intentional interference generated by one or more sources (e.g., Markovian attackers), as the GEO satellite can update the hopping patterns according to previously observed interference. Therefore, it will be difficult for the attackers to keep track of the changes in the frequency-hopping sequences.

In general, two types of transport channels are used in SATCOM systems: dedicated channel (DCH) and random access channel (RACH) [15]. RACH is mainly used for signaling, whereas DCH is commonly used for both data communication and signaling. DCH is similar to our frequency-hopping approach in that each user is assigned an orthogonal code, and thus no two links share the same channel at the same time slot. To ensure correct reception of packets, improve reliability, and reduce packet losses, transmitted packets can be ACKed in RACH. This is feasible when the distance between the transmitter and the receiver is relatively small. However, the distance between LEO and GEO satellites is 33000 kilometers in the best case, which translates into a round-trip time (RTT) of around 0.22 seconds. Such a large RTT would result in a significant communication delay. For that reason, RACH is not commonly used for data transmission in SATCOM.

We now discuss the system architecture in more detail. Consider a network of M LEO satellites that communicate with a common GEO satellite (see Figure 1). The GEO satellite relays data from the LEO satellites to Earth and is capable of performing multi-user FH communications with various LEO satellites. We focus on the "uplink" transmission (from LEO satellites to the GEO satellite), considering a regenerative payload, i.e., the received payload is first decoded and then regenerated by the GEO satellite. Our problem formulations in Section 3 include a constraint that accounts for the minimum SINR requirement for successfully decoding received packets. However, our scheme can also be applied to a bend-pipe relay satellite system by simply removing the SINR constraints in the formulated problems in Section 3.

A sniffer residing within the CR module at the GEO satellite is used to simultaneously detect the energy over several channels that are not being used for transmission at that moment. The sensing outcome allows the GEO satellite to predict the future states of these sensed channels, and update the FH sequences, Tx powers and modulation and coding schemes (MCS). The new assignments are then reported back to the LEO satellites over a feedback channel. The time lag between the current time and the time that the monitored channel will be used for transmission must be large enough to allow for the feedback message to be received at the LEO satellite. By focusing on *future* frequencies in the FH sequence, our approach prevents transmissions over channels with high interference and increases the throughput while minimizing unnecessary energy consumption.

Consider a given uplink that is associated with a *nominal FH sequence*. This sequence is also known to the receiving GEO satellite. Let T be the duration of one slot (time spent transmitting at a given frequency). We assume that T equals to the transmission duration of one or more packets. Let $f_j(n)$ denote the frequency assigned to link j in a given time slot n. The GEO satellite has several

DOI: 10.1002/sat

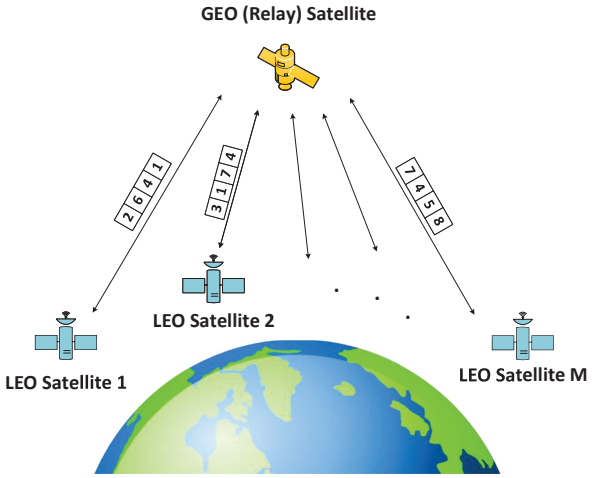

Figure 1. Representative topology of the underlying satellite-to-satellite communications system.

RF chains that are used for concurrent reception of uplink transmissions (on different frequencies) as well as out-of-band sensing of currently unused frequencies. Let T_s be the time spent on sensing a given channel (i.e., the sensing time). Typically, $T_s \ll T$; T_s is usually in the order of tens of milliseconds, whereas $T \sim 100$'s of milliseconds or more [5]. Without loss of generality, we assume $T = CT_s$ for some integer C. Finally, let $\mathcal{J}$ denote the set of all links and $\mathcal{I}$ denote the set of sensed channels at a given time.

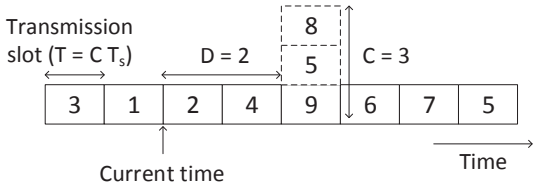

Figure 2. Proactive sensing of "future" frequencies (D = 2, C = 3, single uplink case).

Now, consider an arbitrary time slot n. During that time slot, LEO satellite j and the GEO satellite will be tuned to frequency $f_j(n)$. At the beginning of the slot, the GEO satellite senses channel $f_j(n+D)$ along with $C-1$ other channels, where D (in slots) is the *lag parameter*. For LEO satellite j, if a channel with the desired quality cannot be found (i.e., the minimum SINR cannot be met), the receiver will instruct the transmitter to stay silent during slot $n+D$, so as not to waste energy. The design parameters are explained through the example in Figure 2. The lag parameter allows for adequate time to report back the outcome of the sensing process. This time is called *the feedback time*, and is denoted by T_f. It enables the transmitter to adjust its hopping sequence, Tx power, and MCS.

Our DFH scheme can be viewed as a special case of multi-frequency time-division multiple access (MF-TDMA) scheme [16], commonly used for uplink satellite channels, in the sense that they both use multiple channels and a time-slotted system. In MF-TDMA, the network control center (NCC) coordinates the communication between a group of satellite terminals sharing a set of carrier frequencies, each of which is divided into time slots. A burst is defined by parameters like the carrier frequency, bandwidth, start time, duration and payload type. These characteristics may change between successive bursts, as long as NCC coordinates synchronization between the transmitter and the receiver. The frequency agility of a terminal can be in terms of long-term frequency tuning or fast burst-to-burst carrier switching, analogous to fast frequency hopping (FFH)

DOI: 10.1002/sat

and slow frequency hopping (SFH). However, there is also a significant difference between our scheme and MF-TDMA. MF-TDMA sets a fixed frequency hopping pattern for each transmission and sticks to it for the rest of the operation. Although this approach tends to work well under random interference, it performs poorly in the presence of persistent interference over specific channels [5, 7]. In contrast, our approach allows the FH sequence to be dynamically adjusted according to channel quality and interference conditions. Note that we still assume that before any transmission takes place, the NCC assigns a predefined FH sequence to each LEO satellite to communicate with the GEO satellite. In short, we build DFH on top of MF-TDMA, as an improvement.

Finally, Doppler shift can add interference to adjacent channels other than the intended channel. To prevent such interference between, we use guard bands. Depending on the satellite location, the signal transmitted by one of the LEO satellites may be shifted upward, while that from another LEO satellite on an adjacent channel may be shifted downward. Allowing a guard band that is equal to the maximum possible Doppler shift would address the resulting adjacent-channel interference. A detailed analysis of the calculation of guard bands can be found in the ITU Recommendation 784 on radio-frequency arrangements for systems of the fixed service operating in a portion of Ka-band frequencies [17].

2.1. Feedback Protocol

The main usage of the CC in our scheme is sending updates to LEO satellites to notify them about the required Tx powers/MCS for the upcoming slot. These messages are not acknowledged. If a LEO satellite does not receive a control packet in time, it transmits over the predefined channel at power $P_{\max}$ and the lowest modulation and coding scheme in order to increase the probability of successful delivery. In that case, the difference between the necessary Tx power to satisfy the link budget and $P_{\max}$ is the wasted power. However, if the GEO satellite switches to a different channel assuming LEO satellite has gotten the control packet, the whole Tx power would be wasted and data packet would be lost.

Inter-satellite links (ISLs) rely on a dependable underlying mechanism to transmit/receive control packets [18–21]. In general, a broadcast control channel (CC) is required for ISLs to coordinate motion, location registration/update, and handover procedures between satellites [22]. For instance, the system in [19] supports standard command-and-control functions transmission at any altitude. The transmitter (mother satellite) is equipped with two transponders for redundancy. Two wide-coverage ISL antennas allow the "mother" satellite to receive data from "children" satellites and to exchange control data for position determination, similar to our system model. Both data and control packet transmissions are operated on the same RF band and using the same protocol. In [21], two physical channels are defined: the physical data channel (PDCH), which is used to carry the data burst, and the physical control channel (PCCH), which is used to carry physical-layer signaling information. PDCH is uniquely determined by its chip rate, spreading factor, and data burst length, whereas the PCCH is uniquely determined by its chip rate. For PCCH, random access or dedicated frequency assignment can be used. A CC is also vital for the communication between the GEO satellite and earth station. As described in ITU recommendation 1594 [23], control communications can be carried out via the same satellite used for data transmission and within the internal protocol structure of the broadcast system.

Considering the above possibilities, in our work we employ a dedicated narrow in-band RF channel, which is used only for low rate control communication. Ideally, the feedback (control) channel should always be available, but we have also studied the effect of an erroneous feedback channel in our simulations.

3. PROBLEM FORMULATION

Almost all SATCOM systems implement uplink power control to limit the equivalent isotropically radiated power (EIRP) or maintain constant power spectrum density over carriers of different

DOI: 10.1002/sat

bandwidth, and reduce interference at receiving satellites [16, 21, 24, 25]. As a result, minimum-power channel assignment has been widely studied both in the context of satellite communications and wireless communications in general. However, to the best of our knowledge, it has not been studied in the context of improving a frequency-hopping system. In Section 3.1, we study the minimum-power channel assignment problem without considering the overhead of altering the pre-defined frequency hopping sequences.

In addition, as we consider communications between the LEO and GEO satellites, ISLs are not always available due to high mobility. Therefore, when the link is available (e.g., LEO satellites are close to the GEO satellite), each LEO satellite requires a relatively high data rate to transmit all of the data it collected to the GEO satellite. One example is Earth observation LEO satellites that are specifically designed for non-military uses (e.g., environmental monitoring and meteorology [26]). Environmental and meteorological conditions change dynamically [27], and thus, it is vital for the LEO satellites to transmit the collected data in a timely manner. Therefore, in Section 3.2, we study a rate-maximizing channel assignment problem that such scenarios apply to. In general, the modulation and coding to be used in a time slot can be selected independently, allowing per-time-slot adaptive modulation and coding schemes for more granular and more flexible link adaptation [16].

The main difference between this paper and the previous literature is that, while studying the aforementioned channel assignment problems, we also consider the FH capabilities of the satellites, as in MF-TDMA. Specifically, in Section 3.4, we form combined optimization problems, taking into account the overhead resulting from altering the pre-defined FH sequences (as they will require successful transmission and reception of control packets). We formulate two optimization problems: one aiming at jointly minimizing the normalized total Tx power and the normalized overhead resulting from modifying the FH sequences from their nominal patterns (DFH-Power), and the other aiming at maximizing a weighted difference of the normalized total achievable rate and normalized total overhead (DFH-Rate). For both formulations, we add constraints to ensure that a minimum rate demand for each LEO satellite is satisfied, if such channel assignment is possible (the assignment may not be possible if the best available channel cannot satisfy the link budget of some LEO satellites). For this purpose, we define an SINR threshold, SINR_{th}, and ensure that the SINR at the GEO satellite never goes below that threshold in all channels occupied by the LEO satellites. SINR_{th} can be set to the minimum SINR required for successful communication or to achieve a certain QoS for a given application. This way, different QoS needs of different applications can be accommodated.

3.1. Tx Power Minimization Problem

We first study the minimum-power channel assignment problem. Let $P_j^{(i)}$ denote the Tx power of LEO satellite j when communicating over channel i. The determination of $P_j^{(i)}$ will be discussed in Section 5. $P_j^{(i)}$ must be lower than the maximum allowed Tx power $P_{\max}$. The goal here is to minimize the total Tx power of the LEO satellites, while ensuring that all LEO satellites are assigned channels such that their SINR requirements are met. The problem can be formulated as:

$$
\begin{aligned}
\underset{\{\alpha_j^{(i)}:\, i\in\mathcal{I},\, j\in\mathcal{J}\}}{\text{minimize}} \quad & \pi_{power} \stackrel{\text{def}}{=} \sum_{i=1}^{C}\sum_{j=1}^{M} \alpha_j^{(i)} P_j^{(i)}(\alpha) \\
s.t. \quad & \text{SINR}_j^{(i)} \geq \alpha_j^{(i)} \text{SINR}_{th}, \quad \forall j \in \mathcal{J}, \forall i \in \mathcal{I} \\
& 0 \leq P_j^{(i)} \leq P_{\max}, \quad \forall j \in \mathcal{J}, \forall i \in \mathcal{I} \\
& \sum_{j=1}^{M} \alpha_j^{(i)} \leq 1, \quad \forall i \in \mathcal{I} \\
& \sum_{i=1}^{C} \alpha_j^{(i)} \leq 1, \quad \forall j \in \mathcal{J}
\end{aligned}
\tag{1}
$$

Prepared using satauth.cls
DOI: 10.1002/sat

where $\text{SINR}_j^{(i)}$ is the SINR of LEO satellite j when it uses channel i for transmission, SINR_{th} is the minimum SINR that needs to be met for successful transmission, $\mathcal{J} = \{1, \cdots, M\}$, $\mathcal{I} = \{1, \cdots, C\}$, $\alpha_j^{(i)}$ is a binary variable defined as

$$\alpha_j^{(i)} = \begin{cases} 1, & \text{if channel } i \text{ is assigned to LEO satellite } j \\ 0, & \text{otherwise} \end{cases}$$

and $\alpha = \{\alpha_j^{(i)} : \forall i \in \mathcal{I}, \forall j \in \mathcal{J}\}$. Notice that the optimization needs to be rerun at each time slot. For the sake of clarity, we omit the time index, and consider an arbitrary time slot.

3.2. Rate Maximization Problem

As an alternative formulation for the channel assignment problem, we allow the transmitting LEO satellites to adjust their transmission rates (via modulation and coding) as well as frequencies on a per-hop basis. With the goal of maximizing the total rate, while meeting the SINR requirements of all LEO satellites, we can formulate the problem as:

$$\begin{aligned} \underset{\{\alpha_j^{(i)}:\, i\in\mathcal{I},\, j\in\mathcal{J}\}}{\text{maximize}} \quad & \pi_{rate} \overset{\text{def}}{=} \sum_{i=1}^{C}\sum_{j=1}^{M} \alpha_j^{(i)} R_j^{(i)}(\alpha) \\ s.t. \quad & \text{SINR}_j^{(i)} \geq \alpha_j^{(i)} \text{SINR}_{th}, \quad \forall j \in \mathcal{J}, \forall i \in \mathcal{I} \\ & 0 \leq P_j^{(i)} \leq P_{\max}, \quad \forall j \in \mathcal{J}, \forall i \in \mathcal{I} \\ & \sum_{j=1}^{M} \alpha_j^{(i)} \leq 1, \quad \forall i \in \mathcal{I} \\ & \sum_{i=1}^{C} \alpha_j^{(i)} \leq 1, \quad \forall j \in \mathcal{J} \end{aligned} \tag{2}$$

where $R_j^{(i)}$ is the rate that link j achieves when communicating through channel i and $R_{\max}$ is the maximum possible rate. $R_j^{(i)}$ is a function of the *estimated* interference power on channel i.

3.3. Overhead Minimization Problem

Modifying the nominal FH sequences of LEO satellites in order to minimize the Tx powers (or maximize the transmission rates) increases the feedback overhead. Accordingly, the network designer may be interested in minimizing the number of changes in the nominal FH sequences while meeting the SINR requirements of LEO satellites. Such an optimization problem can be defined as:

$$\begin{aligned} \underset{\{\alpha_j^{(i)}:\, i\in\mathcal{I},\, j\in\mathcal{J}\}}{\text{minimize}} \quad & \pi_{overhead} \overset{\text{def}}{=} \sum_{i=1}^{C}\sum_{j=1}^{M} \alpha_j^{(i)} \mathbb{1}[i \neq f_{j,nom}] \\ s.t. \quad & \text{SINR}_j^{(i)} \geq \alpha_j^{(i)} \text{SINR}_{th}, \quad \forall j \in \mathcal{J}, \forall i \in \mathcal{I} \\ & 0 \leq P_j^{(i)} \leq P_{\max}, \quad \forall j \in \mathcal{J}, \forall i \in \mathcal{I} \\ & \sum_{j=1}^{M} \alpha_j^{(i)} \leq 1, \quad \forall i \in \mathcal{I} \\ & \sum_{i=1}^{C} \alpha_j^{(i)} \leq 1, \quad \forall j \in \mathcal{J} \end{aligned} \tag{3}$$

where $f_{j,nom}$ is the nominal frequency assigned to link j.

DOI: 10.1002/sat

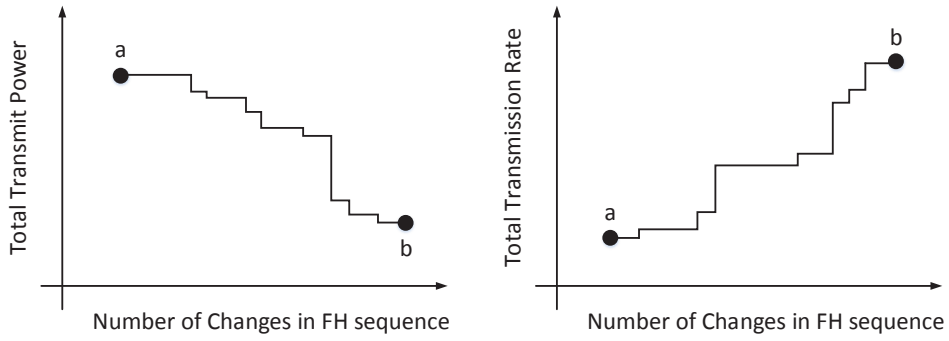

(a) Extreme points in DFH-Power (b) Extreme points in DFH-Rate

Figure 3. Tradeoff between power power minimization/rate maximization and overhead minimization.

3.4. Combined Formulations

The objective functions in (1), (2) and (3) result in different channel assignments. The tradeoff between different objectives can be observed in Figure 3. In Figure 3(a), at point a, $\alpha_j^{(i)}$s are selected in a way to minimize the number of changes in the nominal FH sequences. To meet the minimum SINR constraints, some changes in nominal sequences may still be needed. As a result, the total transmit power will be high. On the other hand, at point b, channel assignment is made such that the total transmit power is minimum, resulting in significant changes in the nominal FH sequence. Similarly, in Figure 3(b), at point a, the changes in the nominal FH sequence are minimized but the total transmission rate is low. At point b, the transmission rate is the highest at the expense of many changes in the FH sequence.

Our main goal is to ensure that all satellites are assigned channels such that their SINR requirements are satisfied. At the same time, in the first cpmbined formulation, we aim at jointly minimizing the total Tx power and the overhead resulting from modifying the FH sequences from their nominal patterns. We call this method as DFH-Power algorithm.

To convert the multi-objective minimization problem into a single-objective one, we use the scalarization technique [28]. For that purpose, we introduce an auxiliary variable β, $0 \leq \beta \leq 1$, and formulate the problem as

$$\begin{aligned}
\underset{\{\alpha_j^{(i)}:\, i\in\mathcal{I},\, j\in\mathcal{J}\}}{\text{minimize}} \quad & \left(\frac{\beta}{P_{\max}M}\pi_{power} + \frac{(1-\beta)}{M}\pi_{overhead}\right) \\
s.t. \quad & \text{SINR}_j^{(i)} \geq \alpha_j^{(i)}\text{SINR}_{th}, \quad \forall j \in \mathcal{J}, \forall i \in \mathcal{I} \\
& 0 \leq P_j^{(i)} \leq P_{\max}, \quad \forall j \in \mathcal{J}, \forall i \in \mathcal{I} \\
& \sum_{j=1}^{M} \alpha_j^{(i)} \leq 1, \quad \forall i \in \mathcal{I} \\
& \sum_{i=1}^{C} \alpha_j^{(i)} \leq 1, \quad \forall j \in \mathcal{J}
\end{aligned} \tag{4}$$

The first term of the objective function represents the normalized sum of assigned Tx powers and the second term represents the normalized total number of changes in the nominal FH sequences. The first constraint ensures that the link budget is enough to support communication while the second constraint imposes an upper bound on the Tx power. The last two constraints ensure that each LEO satellite is assigned exactly one channel.

The parameter β represents the relative importance of minimizing the total power versus minimizing the number of changes to the nominal FH sequences. With $\beta = 1$, the proposed

DOI: 10.1002/sat

algorithm tries to minimize Tx powers only, resulting in significant changes in the nominal FH sequence. The problem then reduces (1). If we set β to 0, the algorithm tries to minimize the changes in the FH sequence only, which is equivalent to (2). β can be adjusted according to the requirements of the system, allowing us to operate the points between a and b in Figure 3.

Similarly, we can formulate another combined objective that aims at maximizing a weighted difference of normalized total achievable rate and normalized total overhead. We call this as DFH-Rate algorithm. The resulting formulation can be stated as follows:

$$\begin{aligned} \underset{\{\alpha_j^{(i)}:\, i\in\mathcal{I},\, j\in\mathcal{J}\}}{\text{maximize}} \quad & \left(\frac{\beta}{R_{\max}M}\pi_{rate} - \frac{(1-\beta)}{M}\pi_{overhead}\right) \\ s.t. \quad & \text{SINR}_j^{(i)} \geq \alpha_j^{(i)}\text{SINR}_{th}, \quad \forall j \in \mathcal{J}, \forall i \in \mathcal{I} \\ & 0 \leq P_j^{(i)} \leq P_{\max}, \quad \forall j \in \mathcal{J}, \forall i \in \mathcal{I} \\ & \sum_{j=1}^{M} \alpha_j^{(i)} \leq 1, \quad \forall i \in \mathcal{I} \\ & \sum_{i=1}^{C} \alpha_j^{(i)} \leq 1, \quad \forall j \in \mathcal{J} \end{aligned} \tag{5}$$

Here, all LEO satellites choose $P_{\max}$ for transmission, as they aim to maximize their rates and there is no power minimization in the objective. In DFH-Rate, we also eliminate the slack between $P_{\max}$ and the minimum required transmit power to achieve the same rate when transmitting at $P_{\max}$, as explained in Section 4.

In the event that we cannot find a feasible solution for all links $j \in \mathcal{J}$ during slot $n + D$, we declare outage for the infeasible links and continue transmission for the feasible ones (i.e., the assignments that require a transmission power less than $P_{\max}$). We consider two types of feasible links, first- and second-stage. First-stage feasible links are those that can be supported without exceeding the maximum Tx power. The number of such links can be found by subtracting the number of outages from M. Second-stage feasible links, on the other hand, correspond to links that require less than or equal amount of the *predicted* Tx power. Links that experience outage in the first stage are not assigned any Tx power in order to conserve energy. However, links that are feasible in the first stage but infeasible in the second stage (due to varying channel conditions) are assigned Tx powers that are less than or equal to $P_{\max}$, but that power is wasted because the estimated link budget is not enough to support the link under the current (exact) channel conditions.

4. OPTIMIZATION ALGORITHMS

Problems (4) and (5) are integer programming (IP) problems, and hence are NP-hard. In this section, we propose an algorithm to transform these IP problems into maximum weighted perfect bipartite matching problems, which can be solved in polynomial-time using the Hungarian algorithm. Still, obtaining the solution to the channel assignment problem takes a non-negligible time. For that reason, new channel assignments are made ahead of time (D slots prior) to allow enough time for solving the optimization problem and notifying the LEO satellites about new channel assignments.

Without loss of generality, assume $C \geq M$, i.e., the number of sensed channels in each slot is larger than the number of LEO satellites. The DFH-Power algorithm takes as inputs the estimated interference levels on various channels, $P_{\max}$, and SINR_{th}. It returns a set of assigned frequencies as well as the Tx powers to be used over these frequencies. The steps of the DFH-Power algorithm are as follows:

1. **Compute the minimum required powers:** For every link j and channel i, $P_j^{(i)}$ (in dB) can be computed as [29, Section 12.6]:

$$P_j^{(i)} = \text{SINR} + \text{Losses} + P_{N+I} - G_T - G_R \tag{6}$$

DOI: 10.1002/sat

where P_{N+I} is the estimated noise-plus-interference power, G_T and G_R are the transmitter and the receiver antenna gains, respectively; and Losses denote the propagation losses experienced by the signal. Letting SINR $=$ SINR$_{th}$, we can use (6) to compute $P_{j,req}^{(i)}$, which is the minimum Tx power for LEO satellite j to successfully communicate through channel i. Then, we identify the infeasible pairs (i,j) such that $P_{j,req}^{(i)} > P_{\max}$.

2. **Assign link weights and solve the matching problem:** In the bipartite graph that we construct, the set of LEO-GEO links, $\mathcal{J}$, and sensed channels, $\mathcal{I}$, are the two sets of nodes. A node within a set can only be connected to another node from the opposite set. Each edge between any two nodes has an edge weight calculated according to the optimization problems in Section 3. Here, we create $C - M$ additional nodes to represent dummy links and denote this set by $\mathcal{J}_D$. Thus, every element in $\mathcal{I}$ will be connected by an edge to every element in $\mathcal{J} \cup \mathcal{J}_D$ (see Figure 4). The edge that connects element i in $\mathcal{I}$ to an element j in $\mathcal{J} \cup \mathcal{J}_D$ will be assigned a link weight:

$$w_j^{(i)} = \begin{cases} \frac{\beta}{P_{max}} P_{j,req}^{(i)} + (1-\beta)\mathbb{1}[i \neq f_{j,nom}], & \text{if } P_{j,req}^{(i)} \leq P_{\max},\, i \in \mathcal{I},\, j \notin \mathcal{J}_D \\ \Gamma, & \text{if } P_{j,req}^{(i)} > P_{\max}, \text{ or } j \in \mathcal{J}_D \end{cases}$$

where Γ is a very large constant. We try to find the assignment that results in the minimum total weight. This assignment problem can be solved using the well-known Hungarian algorithm [30], which can be executed in polynomial time. The Hungarian algorithm requires a square cost matrix; this is the reason we need to create $\mathcal{J}_D$ dummy nodes.

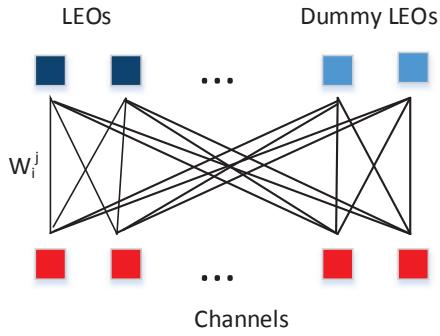

Figure 4. Bipartite graph representing LEO satellite-channel assignments.

The DFH-Rate algorithm takes as input the predicted interference levels on various channels, $P_{\max}$, and rate-versus-SINR function (see Table II). It returns a set of assigned frequencies as well as the MCSs to be used along with these frequencies. For DFH-Rate, we execute the following steps:

1. **Compute maximum achievable rates:** Here, we compute SINR$_j^{(i)}$ by solving (6) for SINR with $P_j^{(i)} = P_{\max}$. Using it, we calculate maximum achievable rates $R_{j,\max}^{(i)} = f(\text{SINR}_j^{(i)})$, where $f(.)$ is the rate-vs-SINR function, exemplified in Table II. Then, we can identify the infeasible (i,j) pairs such that SINR$_j^{(i)} <$ SINR$_{th}$.

2. **Assign link weights and solve the matching problem:** In this step, we assign the link weights that will be used by the Hungarian algorithm as follows:

$$w_j^{(i)} = \begin{cases} -\frac{\beta}{R_{\max}} R_{j,\max}^{(i)} + (1-\beta)\mathbb{1}[i \neq f_{j,nom}], & \text{if SINR}_j^{(i)} \geq \text{SINR}_{th},\, i \in \mathcal{I},\, j \notin \mathcal{J}_D \\ \Gamma, & \text{if SINR}_j^{(i)} < \text{SINR}_{th}, \text{ or } j \in \mathcal{J}_D \end{cases}$$

DOI: 10.1002/sat

Assigning the weights this way and finding the minimum cost assignment is a computationally efficient way of solving the optimization problems in Section 3. We impose the constraints by assigning extremely large weights to infeasible assignments.

3. **Power control:** The Tx power can be reduced below $P_{\max}$ while maintaining the same channel/rate assignment by solving the following problem [31]:

$$\begin{aligned} \text{minimize} \quad & P_j^{(i)} \\ s.t. \quad & f(\text{SINR}_j^{(i)}) = R_{j,max}^{(i)}. \end{aligned}$$

After finding the minimum required powers to achieve the same rate, we add a power margin to the computed Tx powers to compensate for small changes in the predicted channel state.

Table II. Achievable rates for different SINR values

Rate Index	Rate	SINR_{th}	MCS Index
R_1	7.2 Mbps	2	MCS 0
R_2	14.4 Mbps	5	MCS 1
R_3	21.7 Mbps	9	MCS 2
R_4	28.9 Mbps	11	MCS 3
R_5	43.3 Mbps	15	MCS 4
R_6	57.8 Mbps	18	MCS 5
R_7	65 Mbps	20	MCS 6
R_8	72.2 Mbps	25	MCS 7
R_9	86.7 Mbps	29	MCS 8

5. PREDICTING FUTURE CHANNEL CONDITIONS

In this section, we propose a proactive spectrum sensing in which modifications in the nominal FH sequences are based on the future channel conditions, as predicted by the GEO satellite. Markov models have been extensively used to model satellite channels [32–34]. Our Markov model is very robust in the sense that the number of states and the thresholds to partition the received interference into these states can be selected to ensure the best fit to the observations. As discussed previously, our approach is mostly intended for unintentional interference where there is no specific jamming pattern. One common type of interference that can be alleviated by the proposed methods is the one caused by random antenna pointing errors. However, although the proposed approach is not mainly designed to alleviate intentional interference, certain types of adversarial interference (e.g. an attacker that always jams the same channel) can still be accommodated with this approach. Assuming the arrivals of the interfering signals are modulated by a finite-state Markov chain, we can say that the total received interference at the GEO satellite satisfies the Markov property (the past is conditionally independent of the future given the present state of the process) and can therefore be modeled as a discrete-time Markov chain (DTMC). To limit the size of the state space, we follow a common approach in which the interference received by the GEO satellite in each frequency is discretized into a finite number of states. Let the outcome of the sensing process at time n be denoted by Y_n, which represents the total received interference power over a given channel. To quantize Y_n, we introduce a set of threshold values $z_1, z_2, \ldots, z_{q-1}$. Formally, the MC can be defined in terms of:

- **States:** $\mathcal{Q} = \{1, 2, \cdots, q\}$ denote the state space, where state m means that $z_{m-1} \leq Y_n < z_m$, $m \in \mathcal{Q}$.

DOI: 10.1002/sat

- **Transition Matrix:** Transition probability matrix $\mathbf{A}$ of the DTMC consists of q^2 entries $\{a_{ij}\}$, defined as $a_{ij} = \Pr(X_{n+1} = j | X_n = i)$, where X_n is the random variable representing the interference level of a channel at time n.
- **Initial Distribution:** Initially, we assume a uniform distribution $\Pr(X_1 = i) = 1/q,\ \forall i \in \mathcal{Q}$, i.e, all states are equiprobable at time $n = 1$.

The current state of a channel and the transition probabilities between states can be obtained using the sensing results. Using these, the future state of the channel can be predicted. Since our system has a star topology, the common receiver can assign nonoverlapping channels to various transmitters. This way, we make sure that the interference at the receiver will consist of signals from external sources.

The challenge is to generate the DTMC using observation results. Here, the first thing we need to determine is the number of states in the Markov chain. To do that, we partition the received interference powers, sampled at different times, into a set of clusters. For that purpose, we use the well-known k-means centroid algorithm [35]. The input of the k-means algorithm is the interference power of each sample, and the output is the centroid set that represents the mean powers of different clusters of interference samples. The algorithm begins by initializing the cluster centroids randomly. Then, it continuously updates the points assigned to clusters and the new cluster centroids until convergence. k-means is an iterative algorithm in which as the cluster separation increases, the running time decreases and the algorithm's efficiency increases rapidly [36]. Notice that the final results are dependent on the number of clusters k.

One way to select a suitable k is the so-called Elbow method [37]. According to this method, one should choose a number of clusters so that adding another cluster does not give better modeling of the data. One problem with the Elbow method is that it is not quantitative, i.e., it requires an observer to plot the distortion curve and observe the point where the marginal gain drops. Another method to determine the optimum number of clusters is the silhouette analysis. The silhouette value for each point is a measure of how similar that point is to points in its own cluster, when compared to points in other clusters. Formally, the silhouette value for the ith point, S_i, is defined as

$$S_i = \frac{(v_i - u_i)}{\max(v_i, u_i)} \tag{7}$$

where u_i is the average distance from the ith point to the other points in the same cluster as i, and v_i is the minimum average distance from the ith point to points in a different cluster, minimized over clusters. Silhouette values can be used to study the separation distance between the resulting clusters and they have a range of $[-1, 1]$. A silhouette value close to 1 indicates that the sample is far away from the neighboring clusters. A value of 0 indicates that the sample is on or very close to the decision boundary between two neighboring clusters, and negative values indicate that those samples might have been assigned to the wrong cluster. In this paper, to select k, we consider the overall average silhouette width for the entire silhouette plot, which is simply the average $S(i)$ for all objects i in the data set. We then select the k value that gives the largest average silhouette width [38].

Once the number of states are determined and the mean powers of different clusters are obtained, we can then estimate $\mathbf{A}$ of the DTMC. The parameters we wish to infer are the q^2 matrix entries $\{a_{ij}\}$. Here, we use the maximum likelihood estimation (MLE), which is often used to estimate the transition probability matrices of DTMCs, to find an estimator that is consistent with observations [39]. What we observe is a sequence of samples from the chain, $x_1^v \equiv x_1, x_2, \cdots, x_v$, which represents a realization of the random variable X_1^v. The probability of this realization is:

$$\Pr(X_1^v = x_1^v) = \Pr(X_1 = x_1) \prod_{n=2}^{v} \Pr(X_n = x_n | X_1^{n-1} = x_1^{n-1}) \tag{8}$$

$$= \Pr(X_1 = x_1) \prod_{n=2}^{v} \Pr(X_n = x_n | X_{n-1} = x_{n-1}). \tag{9}$$

Prepared using satauth.cls
DOI: 10.1002/sat

While (8) just uses the definition of conditional probability, (9) actually uses the Markov property (that the future is independent of the past, given the present).

To use MLE, we first need to write the likelihood of a given transition matrix as:

$$L(\mathbf{A}) = \Pr(X_1 = x_1) \prod_{n=2}^{v} p_{x_{n-1}x_n}. \tag{10}$$

Define the transition counts matrix $\mathbf{N}$ with entries $\{n_{ij}\}$ as

$$n_{ij} = \sum_{n=2}^{v} \mathbb{1}[X_{n-1} = i, X_n = j] \tag{11}$$

i.e., the number of times a transition occurs from state i to state j in x_1^v. Then, we can rewrite the likelihood in terms of transition counts as:

$$L(\mathbf{A}) = \Pr(X_1 = x_1) \prod_{i=1}^{q} \prod_{j=1}^{q} p_{ij}^{n_{ij}}. \tag{12}$$

Taking the logarithm of this likelihood, we obtain:

$$\mathcal{L}(\mathbf{A}) = \log L(\mathbf{A}) = \log \Pr(X_1 = x_1) + \sum_{i,j} n_{ij} \log p_{ij}. \tag{13}$$

We would like to maximize this log-likelihood w.r.t a_{ij}, subject to the restrictions on the transition probabilities. Formally, we write the problem as:

$$\begin{aligned} \underset{\{a_{ij}\}}{\text{maximize}} \quad & \mathcal{L}(\mathbf{A}) \\ s.t. \quad & a_{ij} \geq 0, \quad \forall i \in \mathcal{Q}, \forall j \in \mathcal{Q} \\ & \sum_{j=1}^{s} a_{ij} = 1, \quad \forall i \in \mathcal{Q}. \end{aligned}$$

To solve this optimization problem using Lagrange multipliers method, we need q Lagrange multipliers $\lambda_1, \lambda_2, \cdots, \lambda_q$. Then, the new objective function becomes

$$\mathcal{L}(\mathbf{A}) - \sum_{i=1}^{j} \lambda_i \left(\sum_{j=1}^{q} a_{ij} - 1 \right). \tag{14}$$

Taking the derivative w.r.t a_{ij} and equating to zero gives

$$\frac{\partial \mathcal{L}(\mathbf{A})}{\partial a_{ij}} = \frac{n_{ij}}{a_{ij}} - \lambda_i = 0 \tag{15}$$

and because $\sum_{j=1}^{q} a_{ij} = 1$, we get

$$\sum_{j=1}^{q} \frac{n_{ij}}{\lambda_i} = 1 \tag{16}$$

$$\sum_{j=1}^{q} n_{ij} = \lambda_i \tag{17}$$

Finally, we can compute the MLE as:

$$\hat{a}_{ij} = \frac{n_{ij}}{\sum_{j=1}^{q} n_{ij}}. \tag{18}$$

Prepared using satauth.cls
DOI: 10.1002/sat

Once the transition probability matrix $\mathbf{A}$ is computed, we calculate the D-step transition matrix $A^{(D)} = A^D$. After that, knowing the current state of the channel and $A^{(D)}$, we estimate the future state of the channel as the state with the highest probability. Then, we can use the estimated interference values in the optimization problems in Section 3. A flowchart of the combined process is given in Figure 5.

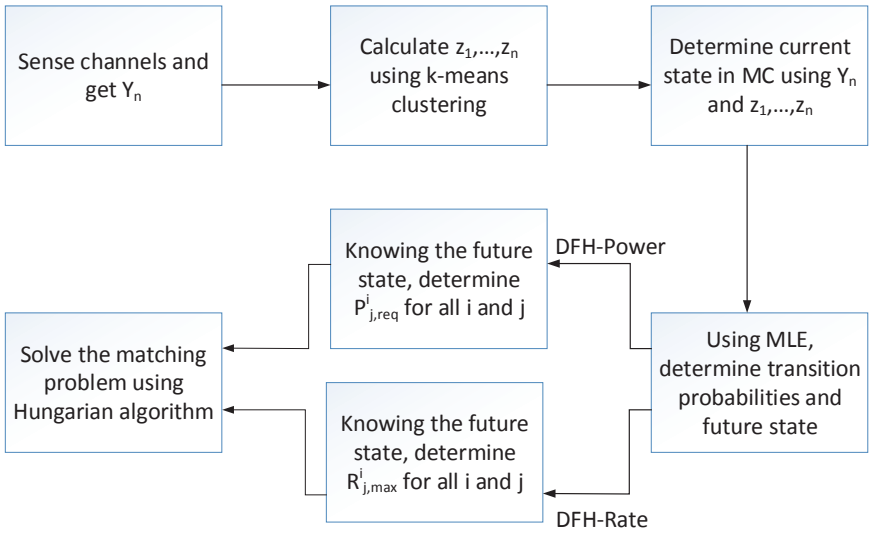

Figure 5. Summary of the proactive sensing and interference mitigation proccess.

6. SIMULATION RESULTS

In this section, we evaluate the performance of the two proposed DFH-Power and DFH-Rate algorithms. The values for key simulation parameters are as follows: number of LEO satellites $M = 20$, number of sensed channels within one transmission slot $C = 100$, distances between LEO satellites and the GEO satellite are uniformly distributed between 33000 and 43000 km, carrier frequency $f_c = 30$ GHz, $P_{\max} = 65$ dBm, $\text{SINR}_{th} = 2$ dB, and the Tx and Rx antenna gains $G_T = G_R = 55$ dBi. To simulate the effect of interference, we assume a total of 10 interferers, where the number of active interferers in each slot follows a birth-and-death process. When active, each interferer generates a random amount of interference, drawn from a Gaussian distribution.

In Figure 6, we investigate the effect of an unreliable feedback channel. For this purpose, we vary the probability of control-packet loss and plot the packet error rates for the DFH-Power and DFH-Rate algorithms. In Figure 6(a), we observe that as the probability of control-packet loss increases, the packet error rate also increases, reaching 1 for $\beta = 1$. With $\beta = 1$, DFH-Power tries to minimize the Tx powers only, resulting in many changes in the nominal FH sequence. If we set β to 0, the algorithm tries to minimize the changes in the FH sequence only, which results in less packet error rate. A similar trend is observed in Figure 6(b) for DFH-Rate. Therefore, in case of an unreliable control channel, we can set β close to 0, meaning that minimizing the changes in the FH sequence is of utmost importance. This way, we can achieve a much lower packet error rate compared to the case with $\beta = 1$. Note that this figure shows the effect of β on packet error rate for an erroneous feedback channel, rather than the actual operating point.

In Figure 7, we study the probability of estimation errors when the future channel state is estimated using the k-means algorithm and MLE. In here, we focus on the case when the estimated channel state is better than the actual state. In this case, the selected Tx power or MCS cannot

DOI: 10.1002/sat

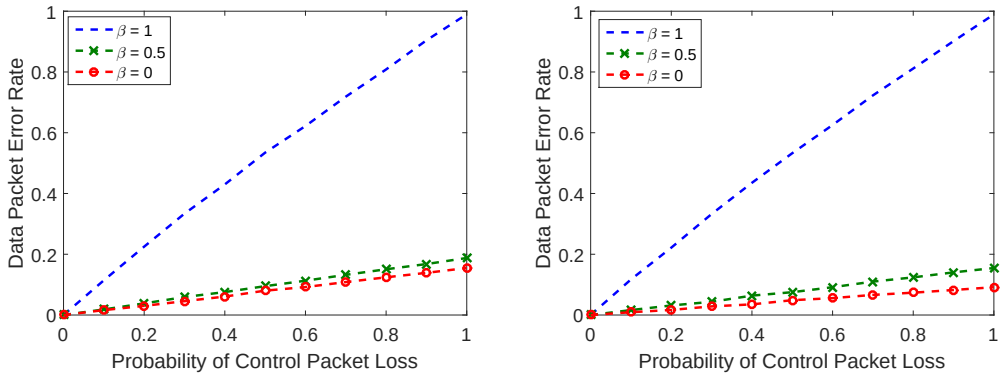

(a) DFH-Power (b) DFH-Rate

Figure 6. Effect of erroneous feedback channel.

support the transmission under the current channel conditions, resulting in a second-stage outage. On the other hand, if the estimated state is worse than the actual state, the LEO and the GEO satellites can still communicate with more Tx power and/or lower MCS index than needed. Note that estimation errors does not necessarily translate into packet errors. When β is close to 0, the algorithms focus on minimizing the changes in the FH sequence rather than optimizing Tx powers or rates. Because links will not be assigned the minimum required powers (for DFH-Power) or maximum MCS indices (for DFH-Rate), state estimation errors may not induce packet errors as in the case with $\beta = 1$. In Figure 7(a), we observe that the error probability increases as D (the lag parameter) increases, since the uncertainty of the estimation increases as the CR tries to estimate farther steps. The increase saturates after some point, as $A^{(D)}$ reaches steady state when $D \to \infty$. On the other hand, as the observation window size increases, more interference samples are acquired, which helps the CR to estimate the transition probabilities more accurately. For that reason, in Figure 7(b), we observe that the error probability decreases as the observation window size increases.

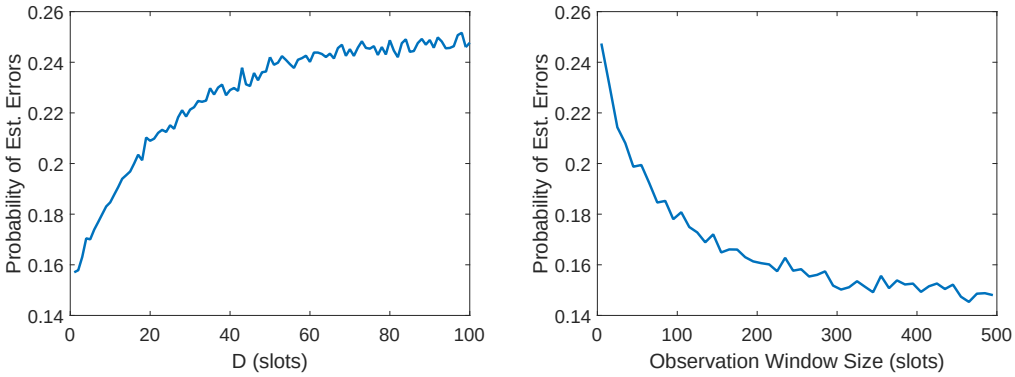

(a) Error probability vs. the lag parameter D (b) Error probability vs. obs. window size

Figure 7. Probability of optimistic estimation errors when the future state is estimated using k-means and MLE.

In Figure 8, we observe that the first-stage outage probability is the same for DFH-Rate and DFH-Power. First-stage outage occurs when the Tx power required to achieve SINR_{th} exceeds $P_{\max}$, and both algorithms aims at satisfying the same SINR constraint. In addition, we observe that the selection of β does not affect the two outage probabilities, because β does not have any effect on the constraints of the underlying optimization problems. Note that when the interference is severe, the second-stage outage probability decreases to zero. The reason is that the first-stage

DOI: 10.1002/sat

outage probability approaches one for severe interference, and second-stage outage can only occur among feasible links that do not experience first-stage outage.

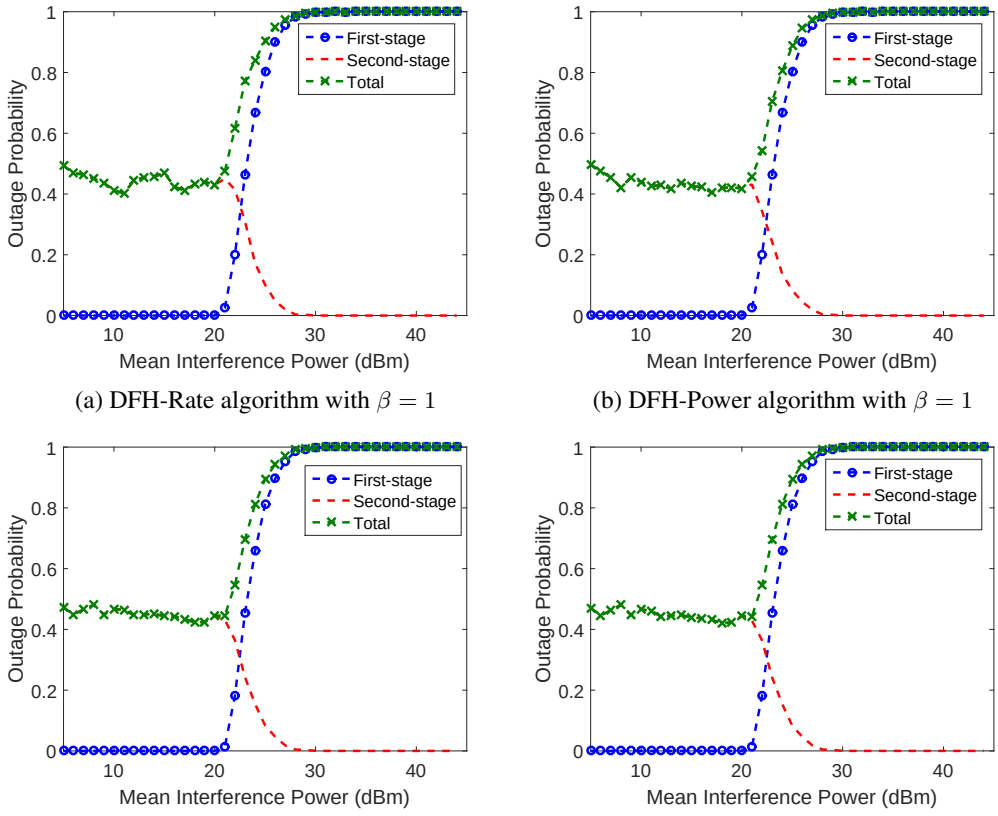

(a) DFH-Rate algorithm with $\beta = 1$

(b) DFH-Power algorithm with $\beta = 1$

(c) DFH-Rate algorithm with $\beta = 0$

(d) DFH-Power algorithm with $\beta = 0$

Figure 8. First-, second-stage and total outage probabilities vs. mean interference powers.

In Figure 9(a), we observe that the achieved throughput of all LEO satellites is much larger under DFH-Rate than under DFH-Power. This is expected since DFH-Rate algorithm has a term for rate maximization in its objective function, whereas DFH-Power algorithm has a term for power minimization. Consequently, in Figure 9(b), we observe that the total Tx power under DFH-Power is less than DFH-Rate. Also, notice that the rates and powers of both algorithms approach zero as the interference power increases. The reason is, as the interference increases, the probability of first-stage outage also increases and the links that are declared in outage are not assigned any power.

In Figure 10(a), we observe that the gap between DFH-Rate and DFH-Power is shrunk when $\beta = 0.5$. This is expected since the objective function in DFH-Rate is no longer solely related to rate maximization. Similar to Figure 10(a), in Figure 10(b), we observe that the gap between the two algorithms is also reduced. Again, this is the attribute to the fact that the objective function for DFH-Power is no longer strictly related to power minimization.

In Figure 11(a), we observe that the gap between DFH-Rate and DFH-Power is further reduced when $\beta = 0$, but still not zero. It is because, even though the objective functions in both algorithms minimize the changes in the nominal FH sequence ($\beta = 0$), the objective function solely affects the channel assignment. After the channel assignment, DFH-Rate assigns LEO satellites powers close to $P_{\max}$, whereas DFH-Power assigns minimum powers that satisfy the SINR constraints. Similar to Figure 11(a), in Figure 11(b), we observe that the gap between DFH-Rate and DFH-Power is shrunk, but is not eliminated.

DOI: 10.1002/sat

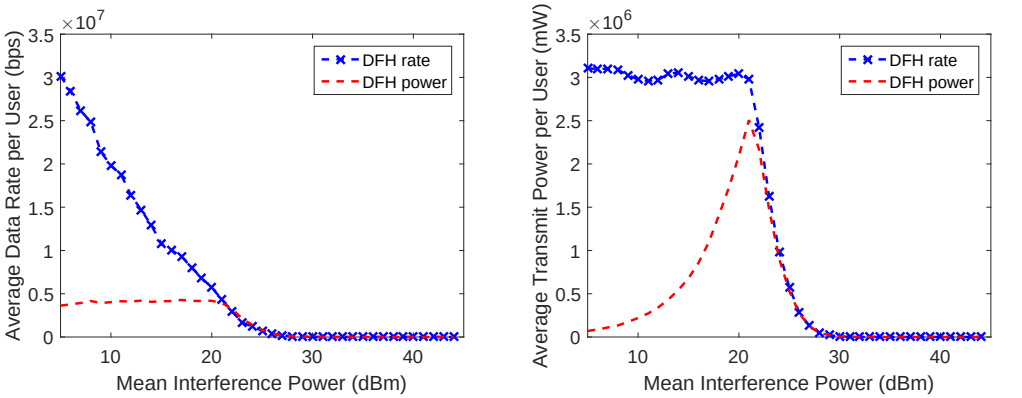

(a) Average rate vs. mean interference power (b) Average power vs. mean interference power

Figure 9. Comparison between DFH-Rate and DFH-Power ($\beta = 1$).

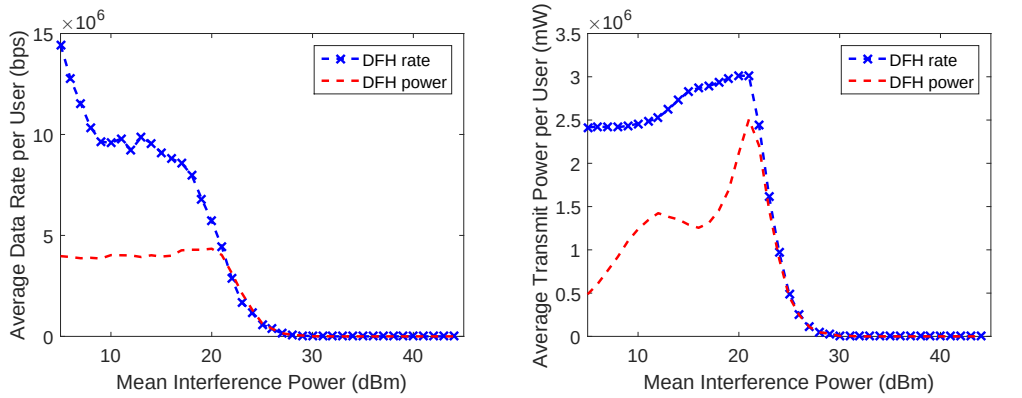

(a) Average rate vs. mean interference power (b) Average power vs. mean interference power

Figure 10. Comparison between DFH-Rate and DFH-Power ($\beta = 0.5$).

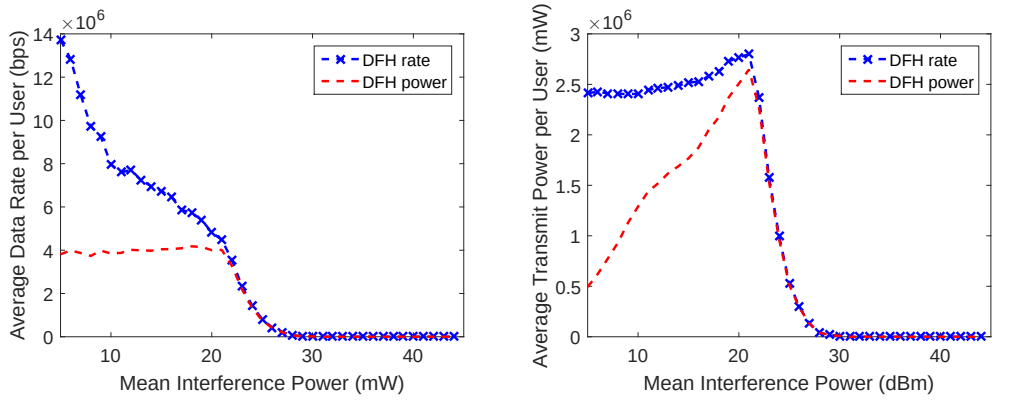

(a) Average rate vs. mean interference power (b) Average power vs. mean interference power

Figure 11. Comparison between DFH-Rate and DFH-Power ($\beta = 0$).

Finally, in Figure 12, we study the effect of β on the total rate and the total consumed power. For small values of β, minimizing the overhead of modifying the nominal FH sequences has more weight on the channel assignment than power/rate optimization. On the other hand, for large β, power minimization and rate maximization are the primary objectives. Consequently, when β is

DOI: 10.1002/sat

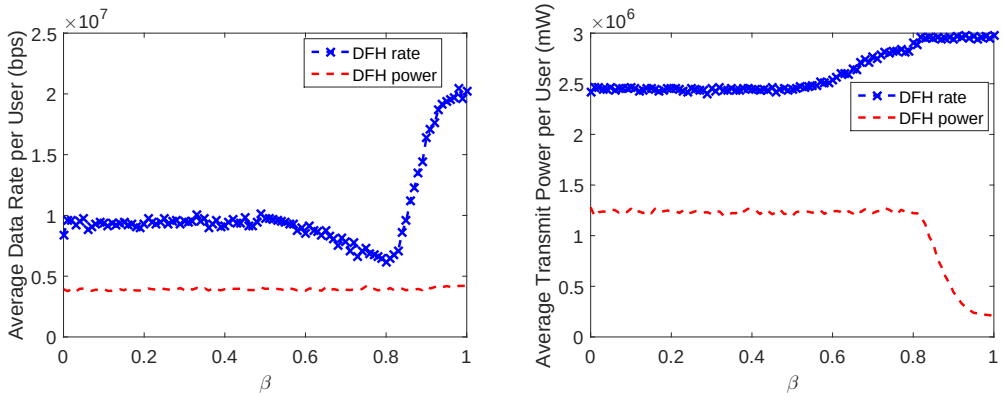

(a) Average rate vs. β. (b) Average power vs. β.

Figure 12. Effect of β on the average data rate and the average Tx power (mean interference power = 10 dBm).

large, the difference between the two algorithms is much larger, both in terms of average data rate and the average Tx power.

7. CONCLUSIONS

In this paper, we proposed two novel dynamic frequency hopping (DFH) approaches, namely, DFH-Rate and DFH-Power, to improve the resilience of SATCOM against intentional and unintentional RF interference. These techniques exploit the sensing capabilities of a cognitive radio module, residing within the receiving satellite, to predict the future interference on upcoming frequencies. We considered multiple LEO satellites as transmitters and a single GEO satellite as the receiver. FH sequences are modified based on predicted interference, taking the total transmit powers, total achievable rates and overhead of modifying the FH sequences into account. In DFH-Power, we aimed at simultaneously minimizing the total Tx power and the changes to the nominal FH sequences while supporting all link transmissions. Considering the large distances between the transmit-receive pairs and the limited lifetime of satellite power sources, minimizing the transmit powers is of utmost importance. In addition, minimizing the changes in the nominal FH sequences is particularly important, when a feedback channel is not always available/reliable. Similarly, in DFH-Rate, the aim was to maximize a weighted difference of the total achievable transmission rate and the overhead of modifying the FH sequences while supporting the maximum number of concurrent transmissions. We studied the tradeoffs between the various terms of the objective functions and proposed a low-complexity solution method based on bipartite matching to solve the two optimization problems. To predict the future channel conditions, we used a Markov chain (MC) and studied a method for estimating the parameters of the MC based on maximum-likelihood estimation (MLE). Finally, we analyzed the effect of system parameters, such as probability of control packet loss, on the performance of the proposed algorithms.

Here, we considered a case where each LEO satellite can only occupy a single (and exclusive) channel at each time slot. As a future work, we plan to extend our treatment, considering more advanced capabilities of satellite radios in such a way that they can occupy M-out-of-K channels. This would require a more complex transceiver hardware, but would also improve interference mitigation.

REFERENCES

1. L. Lightfoot, L. Zhang, and T. Li, “Space-time coded collision-free frequency hopping in hostile jamming,” in *Proceedings of the IEEE MILCOM ’08 Conference*, San Diego, CA, Nov. 2008, pp. 1–7.

DOI: 10.1002/sat

2. D. A. Fritz, D. W. Moy, and R. A. Nichols, "Modeling and simulation of Advanced EHF efficiency enhancements," in *Proceedings of the IEEE MILCOM '99 Conference*, Atlantic City, NJ, Nov. 1999, pp. 354–358.
3. J. Montgomery, D. Runyon, and J. Fuller, "Large multibeam lens antennas for EHF SATCOM," in *Proceedings of the IEEE Military Communications Conference (MILCOM) '88*, San Diego, CA, Oct. 1988, pp. 369–373.
4. R. L. Drummond, M. G. Frick, and F. Denap, "The future of MILSATCOM," in *Proceedings of the International Communication Satellite Systems Conference and Exhibit*, Los Angeles, CA, Mar. 1990.
5. M. J. Abdel-Rahman, M. Krunz, and R. Erwin, "Exploiting cognitive radios for reliable satellite communications," *International Journal of Satellite Communications and Networking*, vol. 33, no. 3, pp. 197–216, 2015.
6. W. Hu, D. Willkomm, M. Abusubaih, J. Gross, G. Vlantis, M. Gerla, and A. Wolisz, "Cognitive radios for dynamic spectrum access - dynamic frequency hopping communities for efficient IEEE 802.22 operation," *IEEE Communications Magazine*, vol. 45, no. 5, pp. 80–87, May 2007.
7. I. Aykin and M. Krunz, "Proactive sensing and interference mitigation in multi-link satellite networks," in *Proceedings of the IEEE GLOBECOM Conference*, Washington D.C., Dec. 2016.
8. D. Cabric, S. M. Mishra, and R. W. Brodersen, "Implementation issues in spectrum sensing for cognitive radios," in *Proceedings of the thirty-eighth Asilomar Conference on Signals, Systems and Computers*. Pacific Grove, CA: IEEE, Jul. 2004, pp. 772–776.
9. T. Yücek and H. Arslan, "A survey of spectrum sensing algorithms for cognitive radio applications," *IEEE Communications Surveys & Tutorials*, vol. 11, no. 1, pp. 116–130, 2009.
10. SWIFT Software Defined Radios. Tethers Unlimited, Inc. [Online]. Available: http://www.tethers.com/SpecSheets/Brochure_SWIFT_SDR.pdf
11. J. M. Nappier and J. C. Briones, "GD SDR automatic gain control characterization testing," 2013. [Online]. Available: https://ntrs.nasa.gov/archive/nasa/casi.ntrs.nasa.gov/20130008206.pdf
12. V. Weerackody and L. Gonzalez, "Motion induced antenna pointing errors in satellite communications on-the-move systems," in *Proc. of the IEEE 40th Annual Conference on Information Sciences and Systems*, 2006, pp. 961–966.
13. A. Raniwala, K. Gopalan, and T.-c. Chiueh, "Centralized channel assignment and routing algorithms for multi-channel wireless mesh networks," *ACM SIGMOBILE Mobile Computing and Communications Review*, vol. 8, no. 2, pp. 50–65, 2004.
14. H. B. Salameh and M. Krunz, "Adaptive power-controlled MAC protocols for improved throughput in hardware-constrained cognitive radio networks," *Ad Hoc Networks*, vol. 9, no. 7, pp. 1127–1139, 2011.
15. European Telecommunications Standards Institute (ETSI), "ETSI TS 102 721-5 V1.2.1 Satellite Earth Stations and Systems; Air Interface for S-band Mobile Interactive Multimedia (S-MIM); Part 5: Protocol Specifications, Link Layer ," 2013. [Online]. Available: http://www.etsi.org/deliver/etsi_ts/102700_102799/10272105/01.02.01_60/ts_10272105v010201p.pdf
16. ——, "ETSI EN 301 545-2 V1.1.1 Digital Video Broadcasting (DVB) Second Generation DVB Interactive Satellite System (DVB-RCS2) Part 2: Lower Layers for Satellite standard ," 2012. [Online]. Available: http://www.etsi.org/deliver/etsi_en/301500_301599/30154502/01.01.01_60/en_30154502v010101p.pdf
17. International Telecommunications Union (ITU), "Recommendation ITU-R F.748-4 Radio-frequency arrangements for systems of the fixed service operating in the 25, 26 and 28 GHz bands ," 2001. [Online]. Available: https://www.itu.int/dms_pubrec/itu-r/rec/f/R-REC-F.748-4-200105-I!!PDF-E.pdf
18. A. Vaneli-Corali, G. E. Corazza, G. Karagiannidis, P. Mathiopoulos, D. Michalopoulos, C. Mosquera, S. Papaharalabos, and S. Sca1ise, "Satellite communications: Research trends and open issues," in *Proceedings of the IEEE International Workshop on Satellite and Space Communications (IWSSC) '07*, Salzburg, Austria, Sep. 2007, pp. 71–75.
19. M. DÉrrico, *Distributed space missions for earth system monitoring*. Springer Science & Business Media, 2012, vol. 31.
20. R. Radhakrishnan, W. W. Edmonson, F. Afghah, J. Chenou, R. M. Rodriguez-Osorio, and Q.-A. Zeng, "Optimal multiple access protocol for inter-satellite communication in small satellite systems," in *Proc. of the 4S Small Satellite Systems and Services Symposium*, 2014.
21. European Telecommunications Standards Institute (ETSI), "ETSI TS 102 721-3 V1.1.1 Satellite Earth Stations and Systems; Air Interface for S-band Mobile Interactive Multimedia (S-MIM); Part 3: Physical Layer Specification, Return Link Asynchronous Access ," 2012. [Online]. Available: http://www.etsi.org/deliver/etsi_ts/102700_102799/10272103/01.01.01_60/ts_10272103v010101p.pdf
22. R. E. Sheriff and Y. F. Hu, *Mobile satellite communication networks*. John Wiley & Sons, 2003.
23. International Telecommunications Union (ITU), "RECOMMENDATION ITU-R S.1594 Maximum emission levels and associated requirements of high density fixed-satellite service earth stations transmitting towards geostationary fixed-satellite service space stations in the 30 GHz range," 2002. [Online]. Available: https://www.itu.int/dms_pubrec/itu-r/rec/s/R-REC-S.1594-0-200209-I!!PDF-E.pdf
24. ——, "Recommendation ITU-R S.1694 Maximum emission levels and associated requirements of high density fixed-satellite service earth stations transmitting towards geostationary fixed-satellite service space stationsin the 30 GHz range ," 2002. [Online]. Available: https://www.itu.int/dms_pubrec/itu-r/rec/s/R-REC-S.1594-0-200209-I!!PDF-E.pdf
25. A. M. Monk and L. B. Milstein, "Open-loop power control error in a land mobile satellite system," *IEEE Journal on Selected Areas in Communications*, vol. 13, no. 2, pp. 205–212, 1995.
26. H. Riebeek, "NASA Earth Observatory," 2009. [Online]. Available: earthobservatory.nasa.gov
27. Z. Renhe, Q. Li, and R. Zhang, "Meteorological conditions for the persistent severe fog and haze event over eastern china in january 2013," *Science China Earth Sciences*, vol. 57, no. 1, pp. 26–35, 2014.
28. C. A. C. Coello, G. B. Lamont, D. A. Van Veldhuizen *et al.*, *Evolutionary algorithms for solving multi-objective problems*. Springer, 2007, vol. 5.
29. D. Roddy, *Satellite communications*. McGraw-Hill, 2006.
30. H. W. Kuhn, "The Hungarian method for the assignment problem," *Naval Research Logistics Quarterly*, vol. 2, no. 1-2, pp. 83–97, 1955.

31. M. Krunz and D. Manzi, "Channel access and traffic control for dynamic-spectrum networks with single-transmit, dual-receive radios," *Computer Communications*, vol. 34, no. 8, pp. 935–947, 2011.
32. F. Babich, G. Lombardi, and E. Valentinuzzi, "Variable order Markov modelling for LEO mobile satellite channels," *Electronics Letters*, vol. 35, no. 8, pp. 621–623, April 1999.
33. B. Vucetic and J. Du, "Channel modeling and simulation in satellite mobile communication systems," *IEEE Journal on Selected Areas in Communications*, vol. 10, no. 8, pp. 1209–1218, 1992.
34. F. P. Fontán, M. Vázquez-Castro, C. E. Cabado, J. P. Garcia, and E. Kubista, "Statistical modeling of the LMS channel," *IEEE Transactions on Vehicular Technology*, vol. 50, no. 6, pp. 1549–1567, 2001.
35. J. A. Hartigan and M. A. Wong, "Algorithm as 136: A k-means clustering algorithm," *Journal of the Royal Statistical Society. Series C (Applied Statistics)*, vol. 28, no. 1, pp. 100–108, 1979.
36. T. Kanungo, D. M. Mount, N. S. Netanyahu, C. D. Piatko, R. Silverman, and A. Y. Wu, "An efficient k-means clustering algorithm: Analysis and implementation," *IEEE Transactions on Pattern Analysis and Machine Intelligence*, vol. 24, no. 7, pp. 881–892, 2002.
37. C. A. Sugar, L. A. Lenert, and R. A. Olshen, "An application of cluster analysis to health services research: Empirically defined health states for depression from the sf-12," Division of Biostatistics, Stanford University, Stanford, CA, Tech. Rep., 1997.
38. P. J. Rousseeuw, "Silhouettes: a graphical aid to the interpretation and validation of cluster analysis," *Journal of Computational and Applied Mathematics*, vol. 20, pp. 53–65, 1987.
39. M. L. Boas, *Mathematical methods in the physical sciences*. Wiley New York, 1966, vol. 2.

DOI: 10.1002/sat